DALTON
FULL PAPER

Neutron-diffraction study of the Jahn–Teller transition in $PrMnO_3$

D. Sánchez,* J. A. Alonso and M. J. Martínez-Lope

Instituto de Ciencia de Materiales de Madrid, C.S.I.C., Cantoblanco, E-28049 Madrid, Spain

Received 27th August 2002, Accepted 3rd October 2002
First published as an Advance Article on the web 1st November 2002

The stoichiometric perovskites $RMnO_3$ (R = rare earth) experience Jahn–Teller (JT) transitions as a function of temperature and R size similar to that recently described for $LaMnO_3$. We have investigated the JT transition for R = Pr by ATD techniques and neutron powder diffraction. This transition takes place at approximately 1050 K, and it is characterized by a strong reduction of the MnO_6 octahedra and sudden changes in the unit cell parameters and Mn–O bond distances. For $T < T_{JT}$, $PrMnO_3$ perovskite exhibits the so-called *O′* orthorhombic structure, characterized by $c/\sqrt{2} < a < b$ and a strong distortion of the MnO_6 octahedra. Also Mn–O distances lying in the basal plane are drastically different, reflecting the orbital ordering due to the JT effect. For $T > T_{JT}$, we observe an orthorhombic *O*-type structure, with much less distorted MnO_6 octahedra and $a < c/\sqrt{2} < b$. In contrast to $LaMnO_3$, the lattice parameters do not converge to give a metrically cubic unit cell above the transition, probably due to the higher mismatch between ionic radii (steric effect)

Introduction

It has been broadly reported that strong correlations between structural and magnetic degrees of freedom in the manganese perovskites give rise to a very rich exhibition of physical phenomena.[1] Among them, the colossal magnetoresistance found in high quality thin films[2] generated a huge amount of scientific work on these materials. Apart from the study of solid solutions of the type $La_{1-x}Ca_xMnO_3$,[3] $Pr_{1-x}Ca_xMnO_3$,[4] $La_{1-x}Sr_xMnO_3$,[5] $Pr_{1-x}Ba_xMnO_3$,[6] and $Pr_{1-x}K_xMnO_3$[7] part of the interest has been centered on the study of undoped compounds, specially the stoichiometric $RMnO_3$ with *Pbnm* orthorhombic structure.

The *O′*-type orthorhombic structure adopted by $RMnO_3$ is a variant of the *O*-type structure with a more distorted MnO_6 octahedra due to the Jahn–Teller (JT) effect of Mn^{3+}.[8] The JT distortion is such that the long and short Mn–O bonds lie in the octahedron basal plane, giving the well known pattern of antiferrodistorsive orbital ordering. It has recently been reported that $LaMnO_3$ undergoes a structural phase transition at T_{JT} = 750 K, above which the orbital ordering disappears.[9] There is no change in symmetry although the lattice becomes metrically cubic on the high-temperature side. The MnO_6 octahedra become nearly regular above T_{JT}, and the thermal parameter of oxygen significantly increases, probably as a result of dynamic spatial fluctuations. However, the behavior of other members of the $RMnO_3$ series has been much less studied. There are hardly any reports of the crystal structure of $PrMnO_{3+\delta}$ (showing oxidative non-stoichiometry),[10] and accurate structural parameters of stoichiometric $RMnO_{3.00}$ for Pr or smaller rare-earth cations have not been reported until recently.[11]

In our experiment we aimed to study the analogous JT transition in $PrMnO_3$, investigating the high temperature evolution of the structural parameters. To do this, we have collected a set of high resolution neutron powder diffraction data at increasing temperatures, on well crystallized stoichiometric $PrMnO_3$ prepared by soft chemistry procedures.

Results

$PrMnO_3$ was obtained as a black, well crystallized powder. From the thermal analysis experiment under reducing conditions, the oxygen content was determined to be 3.02(2); no oxygen excess was detected, within experimental errors. This result seems to exclude the presence of Mn^{4+} in the material, suitably prepared by high temperature annealing under an inert atmosphere. The RT laboratory XRD diagram is characteristic of a single phase, distorted perovskite showing sharp, well defined superstructure reflections, which could be indexed in the conventional *Pbnm* orthorhombic model, with unit-cell parameters related to a_0 (ideal cubic perovskite, a_0 = 4 Å) as $a \approx \sqrt{2}a_0$, $b \approx \sqrt{2}a_0$, $c \approx 2a_0$.

An endothermic peak was observed in the ATD curve at 1018 K, corresponding to the JT transition. It is worth noting that T_{JT} very quickly increases with the degree of distortion of the perovskite (for $LaMnO_3$ T_{JT} is 750 K[9]). For more distorted perovskites *e.g.* $TbMnO_3$, the JT transition, if it exists, takes place at temperatures above 1473 K.

The structural refinement of the RT NPD data was performed by taking the already reported structural parameters for $LaMnO_3$ as a starting model.[9] In the *Pbnm* space group, the Pr atoms are placed at 4c (*x*, *y*, 1/4) positions, Mn at 4b (1/2, 0, 0), O1 oxygens at 4c and O2 at 8d (*x*, *y*, *z*) sites. The final atomic coordinates, unit-cell parameters and discrepancy factors for this RT refinement in the orthorhombic model are given in Table 1. Table 2 lists the main interatomic distances and angles. Fig. 1 depicts two projections of the crystal structure, highlighting the tilting of the MnO_6 octahedra. The main Mn–O bond-lengths at RT are also included in Fig. 1.

The NPD diagrams collected above RT in the Nb furnace were also refined by the Rietveld method in the *Pbnm* space group, over all of the temperature ranges. As the presence of Nb peaks from the furnace were detected, Nb metal was refined as a secondary phase. The goodness of the fit at RT (collected outside the furnace) and at a selected temperature above T_{JT} is displayed in Fig. 2. Tables 1 and 2 also include the main crystallographic parameters and interatomic distances and angles at some selected temperatures below and above T_{JT}. It is worth indicating that the refinement of the high temperature phase, above T_{JT}, was also tried in the rhombohedral $R\bar{3}c$ and in the cubic $Pm\bar{3}m$ space groups, leading to much poorer fits of the experimental profile. A second analysis of the oxygen contents of the sample, performed after the NPD data collection at high temperature under dynamic vacuum, showed no departure from the stoichiometric composition within experimental error.

 DOI: 10.1039/b208660n

Table 1 Atomic parameters and agreement factors after the Rietveld refinement of the $PrMnO_3$ crystal structure from NPD data at selected temperatures. The JT transition takes place at T_{JT} = 1050 K

	RT	898 K ($T<T_{JT}$)	1133 K ($T>T_{JT}$)	1263 K
Pbnm				
a/Å	5.4492(1)	5.4861(4)	5.5326(2)	5.5494(2)
b/Å	5.8130(2)	5.7821(3)	5.6176(2)	5.6110(2)
c/Å	7.5856(2)	7.6854(5)	7.8513(3)	7.8730(3)
V/Å^3	240.28(1)	243.79(3)	244.02(2)	245.14(2)
Pr 4c (*x y* ¼)				
x	0.9910(6)	0.990(1)	0.992(1)	0.993(1)
y	0.0639(5)	0.046(1)	0.0350(8)	0.0329(8)
B/Å^2	0.75(4)	1.4(1)	1.75(8)	2.02(9)
Mn 4b (½ 0 0)				
B/Å^2	0.63(3)	0.7(1)	1.05(9)	1.25(9)
O1 4c (*x y* ¼)				
x	0.0834(4)	0.0817(7)	0.0762(7)	0.0764(8)
y	0.4820(4)	0.4847(7)	0.4825(7)	0.4816(7)
B/Å^2	0.74(4)	1.4(1)	2.21(9)	2.69(9)
O2 8d (*x y z*)				
x	0.7151(3)	0.7158(5)	0.7126(5)	0.7136(5)
y	0.3174(3)	0.3161(5)	0.2970(4)	0.2938(5)
z	0.0430(2)	0.0415(4)	0.0416(3)	0.0418(4)
B/Å^2	0.77(3)	1.30(7)	1.92(6)	2.34(7)
Reliability factors				
χ^2	2.13	3.54	3.10	4.01
R_p(%)	4.11	8.54	7.09	6.51
R_{wp}(%)	5.16	11.0	9.30	8.81
R_I(%)	5.27	7.95	7.43	7.50

Table 2 Main interatomic distances (Å) and angles (°) of $PrMnO_3$ at selected temperatures

	RT	898 K ($T < T_{JT}$)	1133 K ($T > T_{JT}$)	1263 K
Pbnm				
Mn–O(1) (*m*)	1.9530(5)	1.9749(9)	2.0100(9)	2.016(1)
Mn–O(2) (*s*)	1.909(2)	1.914(3)	1.984(3)	1.993(3)
Mn–O(2) (*l*)	2.210(2)	2.201(3)	2.067(3)	2.057(3)
Δ (Mn–O) × 10^{-4}	43.021	36.888	2.959	1.717
Mn–O(1)–Mn	152.35(2)	153.25(4)	155.13(4)	154.98(4)
Mn–O(2)–Mn	150.52(6)	151.1(1)	153.4(1)	153.9(1)

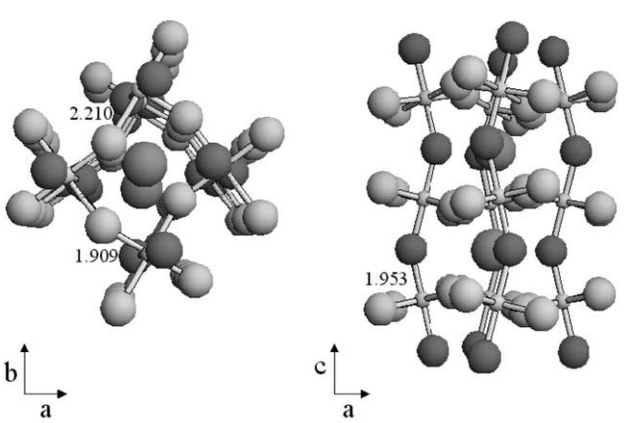

Fig. 1 Two projections of the crystal structure of $PrMnO_3$ at RT. The three Mn–O bond-lengths (Å) are indicated: two Mn–O2 bonds (*short* and *long*) are in the basal *ab* plane; Mn–O1 (*medium*) is the apical bond of the MnO_6 octahedra, in the *Pbnm* description.

Fig. 3 shows the thermal variation of the unit-cell parameters. The three parameters show pronounced changes at T = 1050 K, going from $c/\sqrt{2} < a < b$ to $a < c/\sqrt{2} < b$ when increasing temperature across T_{JT}. Also the Mn–O distances vary abruptly at this temperature. As shown in Fig. 4, long (l = Mn–O(2) × 2), medium (m = Mn–O(1) × 2) and short (s = Mn–O(2) × 2) distances vary slowly at high T (T > 1050 K) and become more different upon lowering the temperature, thus reflecting a more distorted octahedral environment for T < 1050 K. It is worth noting that the Mn–O distances in the *ab* plane (l and s) experience the strongest variation. It is also interesting to quantify the relative distortion of the octahedra by defining the Δ parameter, concerning the deviation of the Mn–O distances with respect to the average <Mn–O> value, as $\Delta = (1/6)\Sigma_{n=1,6}[(d_n - \langle d \rangle)/\langle d \rangle]^2$. At RT, Δ takes a value of 43.1 × 10^{-4}; the strong suppression of the distortion of the oxygen octahedra at T_{JT} is evidenced also in Fig. 5.

The unit cell volume (Fig. 6) behaves in a non-monotonic way. First, there is a unit cell thermal expansion from room temperature to 948 K. Then the system experiences constriction from 948 K to 1050 K and then it expands again up to the highest temperature measured.

Discussion

It is clear from Figs. 3, 4 and 5 that $PrMnO_3$ undergoes a structural phase transition from orthorhombic O'-type to orthorhombic O-type upon increasing the temperature up to 1050 K. The sudden decrease in the MnO_6 octahedral distortion and the convergence of lattice parameters and Mn–O

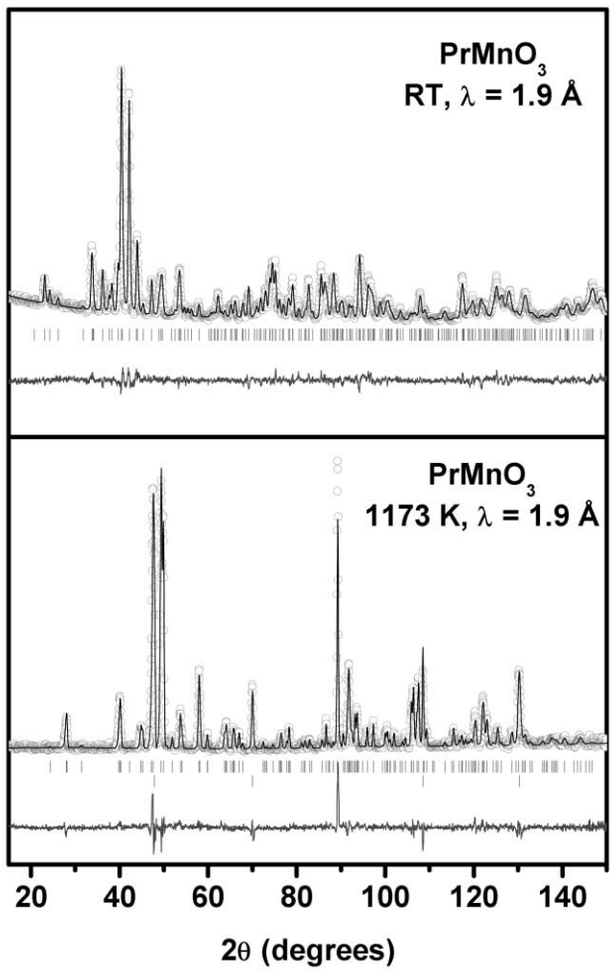

Fig. 2 Rietveld profiles after the refinement of the $PrMnO_3$ crystal structure in the *Pbnm* group from NPD data at selected temperatures, below and above the Jahn–Teller transition (T_{JT} = 1050 K). The vertical lines indicate the allowed Bragg reflections. The second series in the 1173 K pattern corresponds to Nb reflections from the furnace, included as a second crystallographic phase in the refinement.

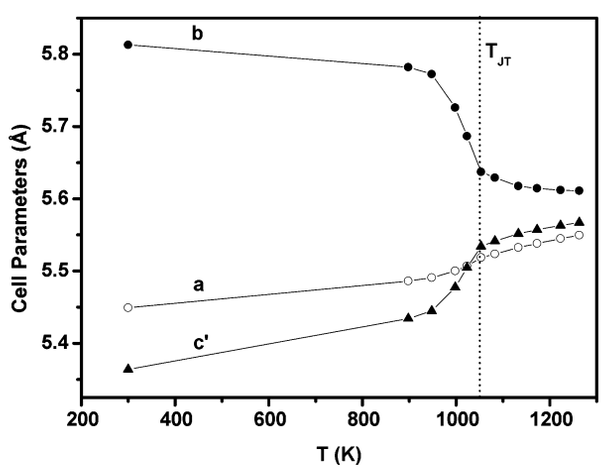

Fig. 3 Thermal variation of the unit cell parameters *a*, *b* and $c/\sqrt{2}$ of $PrMnO_3$.

distances give evidence that the Jahn–Teller distortion and hence the orbital ordering disappear at T_{JT} = 1050 K. It is worth noting how the transition temperature (T_{JT}) rapidly increases with the degree of distortion of the perovskite; that is, when the ionic radius of the rare earth is reduced in $RMnO_3$ compounds.[13] For R = La, a Jahn–Teller transition temperature of 750 K is reported in ref. 9; we obtain T_{JT} = 1050 K for R= Pr and T_{JT} = 1143 K was measured by the ATD techniques for R= Nd.

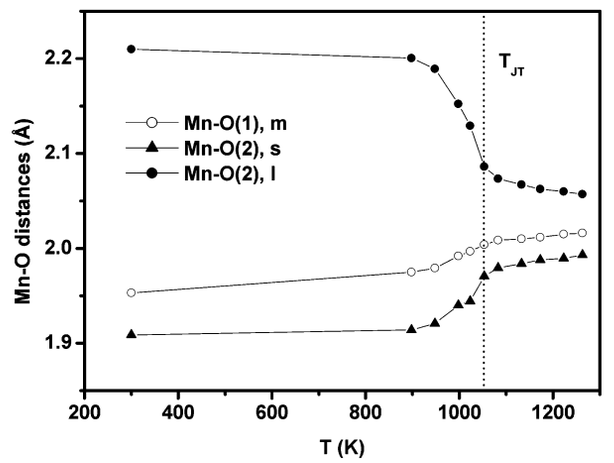

Fig. 4 Thermal variation of medium (*m*), long (*l*) and short (*s*) Mn–O bond distances.

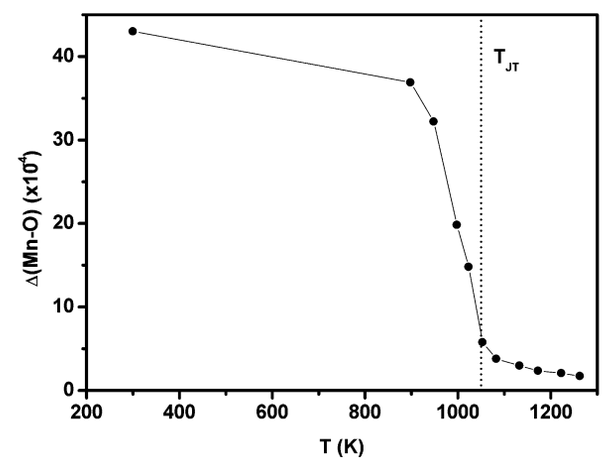

Fig. 5 Strong decrease in the distortion of the MnO_6 octahedra, defined as $\Delta = (1/6)\Sigma_{n=1,6}[(d_n - \langle d \rangle)/\langle d \rangle]^2$, showing the Jahn–Teller transition at 1050 K.

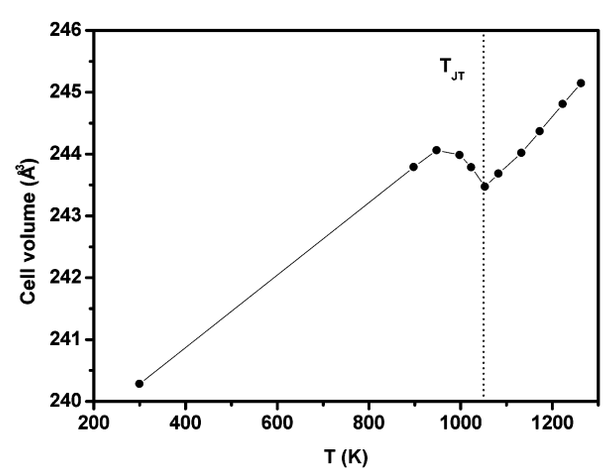

Fig. 6 Non-monotonic behaviour of the unit-cell volume with temperature.

It is interesting to mention some differences between the La and Pr perovskites in the JT transition. First of all, the $LaMnO_3$ lattice becomes metrically cubic in the *O* phase probably due to the dynamic local distortions of the octahedra.[9] Although the same type of spatial fluctuations could be present in the Pr compound, the lattice parameters do not converge to give a metrically cubic unit cell due to the higher mismatch between ionic radii (steric effect). In the *O* phase, in the absence of JT distortions, the fluctuations related to the dynamic JT effect[9] do not overcome the steric effect.

However, it has been reported that the transition from orthorhombic to quasicubic symmetry occurs at higher temperatures. In ref. 4, two subsequent phase transitions are reported for $PrMnO_3$; the first one at 820 K is related to a O'–O structural transition and at the second one, at 945 K, the compound is reported to undergo a structural transition from O-type orthorhombic to quasicubic. As we observe the JT transition at T_{JT} = 1050 K, it is possible that the O-quasicubic transition takes place at a temperature out of our range of measurement. The differences in the transition temperatures could be attributed to stoichiometry defects, which are known to be responsible for the presence of Mn^{4+} in the system. As pointed out in ref. 9, a non-negligible amount of Mn^{4+} is able to substantially shift the temperatures of the two phase transitions.

Conclusions

We have studied the Jahn–Teller transition in $PrMnO_3$ perovskite by NPD measurements at high temperatures. The transition temperature (T_{JT} = 1050 K) is substantially higher than that reported for the La compound (T_{JT} = 750 K), and the unit cell does not become metrically cubic in the O-type orthorhombic phase. It is expected that another transition from orthorhombic (O-type) to quasicubic symmetry occurs at higher temperatures, out of our present range of measurement.

Experimental

Soft chemistry procedures have been employed to prepare the stoichiometric $PrMnO_3$ oxide; inert-atmosphere annealing has been required to avoid the formation of oxidized $PrMnO_{3+\delta}$ phases, thus minimizing the unwanted presence of Mn^{4+}. Stoichiometric amounts of analytical grade Pr_2O_3 and $MnCO_3$ were dissolved in citric acid, by adding several droplets of concentrated HNO_3 to favor the dissolution of the rare-earth oxides. The citrate + nitrate solutions were slowly evaporated, leading to organic resins containing a random distribution of the involved cations at an atomic level. These resins were first dried at 120 °C and then slowly decomposed at temperatures up to 600 °C. All the organic materials and nitrates were eliminated in a subsequent treatment at 700 °C in air, for 12 hours. This treatment gave rise to highly reactive precursor materials, amorphous to X-ray diffraction (XRD). Finally, the precursor was treated at 1100 °C in a N_2 flow for 12 hours.

The product was initially characterized by laboratory XRD for phase identification and to assess phase purity. The oxygen content of the sample was determined by thermal analysis in reducing conditions (H_2(5%)/N_2(95%)flow), through total reduction to MnO + Pr_2O_3, in a Mettler TA3000 system equipped with a TC10 processor unit. Thermogravimetric (TG) curves were obtained in a TG50 unit working at a heating rate of 5 K min^{-1}. A sample of about 50 mg was used. A second analysis of the oxygen content was performed after the high temperature neutron experiment, under the same conditions.

The phase transition was followed by ATD techniques, in a Seiko TG/ATD 320 U, in the temperature range from RT to 1273 K, with a heating rate of 10 K min^{-1}. About 50 mg of $PrMnO_3$ were used in the experiment. Neutron powder diffraction experiments were carried out in the powder diffractometer D1A (λ = 1.90 Å) at the ILL, Grenoble. Data collection took place at RT and at 10 temperatures across the Jahn–Teller transition : 898 K, 948 K, 998 K, 1023 K, 1053 K, 1083 K, 1133 K, 1173 K, 1223 K, 1263 K. About 4 g of $PrMnO_3$ were contained in a vanadium can, set inside a niobium furnace. The temperature was slowly increased, and stabilized for half an hour before each measurement. To avoid hysteresis problems, the collection was always performed in the heating run. Each pattern required 6–8 hours to get sufficiently good statistics.

All the patterns were refined by the FULLPROF Rietveld refinement program.[12] A pseudo-Voigt function was chosen to generate the line shape of the diffraction peaks. The background was fitted with a fifth-degree polynomial function. Since several peaks coming from the niobium furnace were detected in the pattern, the crystal structure of Nb metal was introduced as a second phase in the final refinements, in the patterns collected above RT. Scale factors of $PrMnO_3$ and Nb, background coefficients, zero-point error, unit-cell parameters, positional coordinates, isotropic thermal factors and asymmetry parameters were refined in the final run. The scattering lengths of Pr, Mn and O were 4.580, −3.730 and 5.803 fm, respectively.

Acknowledgements

We thank the ILL for making their neutron diffraction facilities available, and the financial support of CICyT to the projects MAT2001-0539 and MAT99-1045 is acknowledged.

References

1 J. M. D. Coey and M. Viret, *Adv. Phys.*, 1999, **48**, 167.
2 S. Jin, T. H. Tiefel, M. McCormack, R. A. Fastnacht, R. Ramesh and L. H. Chen, *Science*, 1994, **264**, 413.
3 E. O. Wollan and W. C. Koehler, *Phys. Rev.*, 1955, **100**, 545.
4 M. R. Lees, J. Barratt, G. Balakrishnan, D. McK Paul and C. D. Dewhurst, *J. Phys.: Condens. Matter*, 1996, **8**, 2967.
5 H. Kawano, R. Kajimoto, M. Kubota and H. Yoshizawa, *Phys. Rev. B*, 1991, **53**, 2202.
6 Z. Jirak and E. Pollert, *Eur. J. Solid State Inorg. Chem.*, 1990, **27**, 421.
7 Z. Jirak, J. Hejtmanek, K. Knizek and R. Sonntag, *J. Solid State Chem.*, 1997, **132**, 98.
8 J. B. Goodenough, *Magnetism and the Chemical Bond*, Wiley-Interscience, New York, 1996.
9 J. Rodríguez-Carvajal, M. Hennion, F. Moussa, A. H. Moudden, L. Pinsard and A. Revcolevschi, *Phys. Rev. B*, 1998, **57**, R3189.
10 V. A. Cherepanov, L. Yu. Barkhatova, A. N. Petrov and V. I. Voronin, *J. Solid State Chem.*, 1995, **118**, 53.
11 J. A. Alonso, M. J. Martínez-Lope, M. T. Casais and M. T. Fernández-Díaz, *Inorg. Chem.*, 2000, **39**, 917.
12 J. Rodríguez-Carvajal, *Physica B (Amsterdam)*, 1993, **192**, 55.
13 L. Martín-Carrón and A. de Andrés, *J. Alloys Compd.*, 2001, **323–324**, 417.